



LAWRENCE
LIVERMORE
NATIONAL
LABORATORY

Nanoporous gold as a highly active substrate for surface-enhanced Raman scattering spectroscopy

S. O. Kucheyev, J. R. Hayes, J. Biener, A. V. Hamza

March 31, 2006

Applied Physics Letters

Disclaimer

This document was prepared as an account of work sponsored by an agency of the United States Government. Neither the United States Government nor the University of California nor any of their employees, makes any warranty, express or implied, or assumes any legal liability or responsibility for the accuracy, completeness, or usefulness of any information, apparatus, product, or process disclosed, or represents that its use would not infringe privately owned rights. Reference herein to any specific commercial product, process, or service by trade name, trademark, manufacturer, or otherwise, does not necessarily constitute or imply its endorsement, recommendation, or favoring by the United States Government or the University of California. The views and opinions of authors expressed herein do not necessarily state or reflect those of the United States Government or the University of California, and shall not be used for advertising or product endorsement purposes.

Nanoporous gold as a highly active substrate for surface-enhanced Raman scattering spectroscopy

S. O. Kucheyev, J. R. Hayes, J. Biener, and A. V. Hamza
Lawrence Livermore National Laboratory, Livermore, California 94551
(Dated: March 28, 2006)

Colloidal solutions of metal nanoparticles are currently among most studied substrates for sensors based on surface-enhanced Raman scattering (SERS). However, such substrates often suffer from not being cost-effective, reusable, or stable. Here, we develop nanoporous Au as a highly active, tunable, affordable, stable, bio-compatible, and reusable SERS substrate. Nanoporous Au is prepared by a facile process of free corrosion of AgAu alloys followed by annealing. Results show that nanofoams with average pore sizes of ~ 250 nm exhibit the largest SERS signal for 632.8 nm excitation. This is attributed to the electromagnetic SERS enhancement mechanism with additional field localization within pores.

PACS numbers: 61.43.Gt, 68.43.Pq

Surface-enhanced Raman scattering (SERS) spectroscopy probes bond vibrations of molecules in the proximity of metallic nanostructures.¹ This technique has regained considerable interest in recent years stimulated by an explosive development of nanotechnology¹ and superior sensitivity of SERS, in some cases possibly approaching the single molecule detection limit.^{2,3}

Despite numerous previous reports demonstrating the SERS effect for different molecules and substrates, there is still an ongoing search for better substrates for SERS-based chemical sensors.¹ Indeed, colloidal solutions of Au or Ag with particle sizes in the submicron range are currently among most studied SERS-active substrates. However, such substrates are not reusable and, hence, not cost-effective. This fact and the limited stability and reproducibility of metal colloids often hamper their practical use.¹

In this letter, we report on the development of nanoporous Au (*np*-Au) as a highly active, stable, tun-

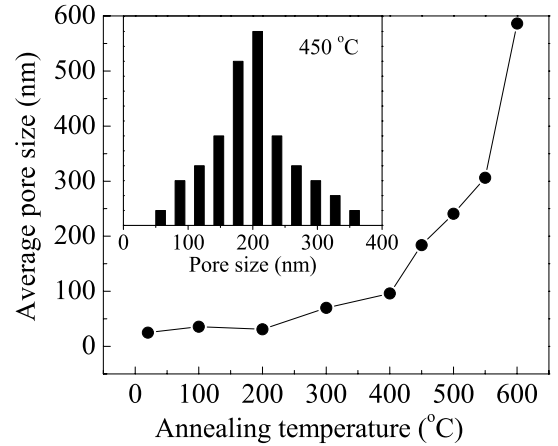


FIG. 2: Dependence of the average pore size on annealing temperature of *np*-Au. The inset shows the distribution of pore sizes in *np*-Au annealed at 450 °C.

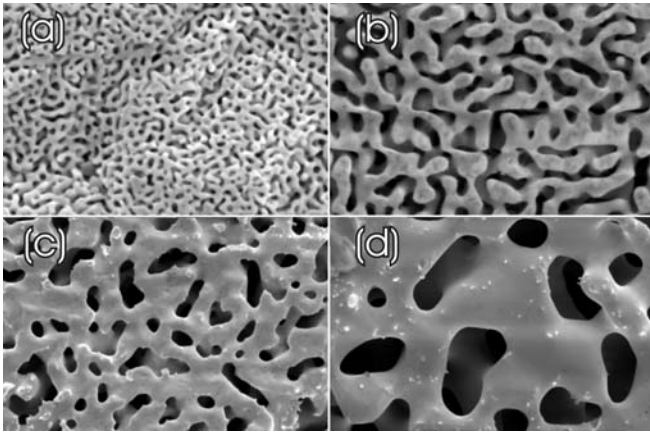


FIG. 1: Typical SEM images (primary electron energy is 5 keV) illustrating the surface morphology of as-dealloyed *np*-Au (a) and *np*-Au annealed for 2 hours at 300 °C (b), 450 °C (c), and 550 °C (d). The horizontal field widths are ~ 2.4 μm for images (a) and (b) and ~ 6.0 μm for images (c) and (d).

able, bio-compatible, reusable, and affordable (particularly when used as a thin nanoporous Au film on a low-cost substrate) SERS substrate. Additional attractiveness of *np*-Au comes from the fact that it is compatible with well-studied self-assembled monolayers of thiols, which can be used as linking layers in advanced sensor applications. We show that the largest SERS enhancement factors, with crystal violet as a test molecule and 632.8 nm laser excitation, are observed for *np*-Au with an average pore size of ~ 250 nm.

Nanoporous Au samples, $\sim 5.0 \times 5.0 \times 0.3$ mm³ in size, were prepared by free corrosion of a Ag_{0.7}Au_{0.3} starting alloy in an ~ 16 molar aqueous solution of HNO₃ for 48 hours at room temperature. Such a procedure results in selective dissolution of Ag and the surface-diffusion-limited self-assembly of the remaining Au atoms into *np*-Au with a relative density of $\sim 30\%$ and an open-

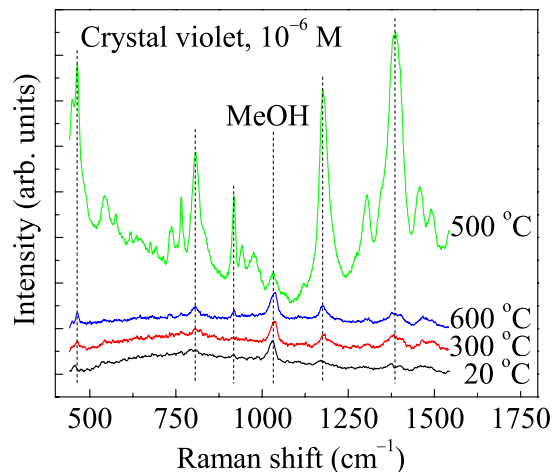


FIG. 3: (Color online) Representative SERS spectra (for a 10^{-6} molar solution of crystal violet) from np -Au annealed at different temperatures, as indicated. Spectra are offset for clarity. A methanol-related peak is labeled “MeOH.”

cell sponge-like morphology with elongated pores with an average width of ~ 25 nm [see a scanning electron microscopy (SEM) image in Fig. 1(a)].

Ligament and pore sizes were tuned by thermal annealing of as-dealloyed foams in an Ar atmosphere for 2 hours in the temperature range of $100 - 600$ $^{\circ}\text{C}$, as illustrated in SEM images of the surfaces of np -Au in Fig. 1 (for selected annealing temperatures of 300 , 450 , and 550 $^{\circ}\text{C}$). The dependence of the average pore size, obtained from statistical analysis of SEM images such as illustrated in Fig. 1, on annealing temperature is shown in Fig. 2. It is seen from Figs. 1 and 2 that, with increasing annealing temperature above ~ 400 $^{\circ}\text{C}$, the size of pores and ligaments rapidly increases. In addition, the aspect ratio of the pores intersecting the sample surface decreases with increasing annealing temperature (i.e., pores and ligaments become less elongated). The inset in Fig. 2 illustrates a relatively wide pore size distribution for a sample annealed at 450 $^{\circ}\text{C}$, which is representative of all the other samples studied here and is consistent with a previous report.⁴

Raman scattering was studied in a Jobin Yvon Raman spectrometer (model HR800) equipped with a He-Ne (632.8 nm) laser as an excitation source. Crystal violet (CV) 10B was used as a test molecule, with methanol as a solvent. After a linear background subtraction, all spectra were normalized to the intensity of a methanol-related Raman band centered on ~ 1035 cm^{-1} . Both (exterior) sample surfaces and cross sections (prepared by simple fracturing since np -Au is macroscopically brittle) revealed overall the same data trends. Hence, in this letter, we will show data from the surfaces only.

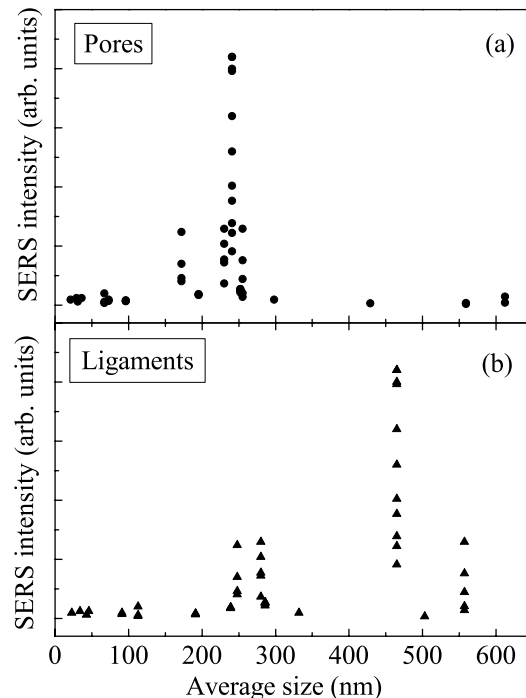


FIG. 4: Dependence of SERS intensity (defined as the integral intensity of the band centered on ~ 1175 cm^{-1}) on the average pore (a) or ligament (b) size. Different data points for the same pore or ligament size represent spectra taken from different areas of the same sample. All data are for a 10^{-6} molar solution of crystal violet.

Figure 3 shows typical SERS spectra from np -Au annealed at different temperatures. These Raman spectra consist of a methanol-related peak centered on ~ 1035 cm^{-1} and a series of CV-related SERS bands. Note that no measurable SERS signal was observed from flat Au surfaces (Au deposited on glass slides) even for the largest CV concentration used (a 10^{-5} molar methanolic solution). It is seen from Fig. 3 that the SERS enhancement strongly depends on the annealing temperature and, hence, on the average size of pores and/or ligaments (see Figs. 1 and 2). In particular, samples annealed at temperatures around 500 $^{\circ}\text{C}$ exhibit the maximum SERS signal.

To better correlate SERS signal enhancement with the morphology of np -Au, Fig. 4 shows the dependence of SERS intensity on the average pore [Fig. 4(a)] or ligament [Fig. 4(b)] size. Note that, in Figs. 4(a) and 4(b), different data points for the same pore or ligament size^{5,6} represent Raman spectra taken from different areas of the same sample. Figure 4(b) reveals no clear correlation between SERS intensity and the average ligament size. For the same set of nanofoams as in Fig. 4(b), however, Fig. 4(a) shows that SERS intensity is maximum for

foams with an average pore size of ~ 250 nm. With this pore size, we could readily detect SERS signal from 10^{-7} molar methanolic solutions of CV. Note that the length scale dependence revealed by Fig. 4 suggests that *np*-Au could be a tunable SERS substrate when the SERS response is optimized for any given excitation source by adjusting the pore size in a straightforward thermal annealing step.

Data from Fig. 4 provides clear evidence that SERS enhancement better correlates with the average pore size rather than with the ligament size. Hence, we attribute efficient SERS from *np*-Au to well-established electromagnetic SERS enhancement mechanism related to an efficient excitation and trapping of surface plasmons and the geometrical “lightning rod” effect,¹ but with an additional effect of field localization in the pore regions. Our experimental finding is, qualitatively, consistent with several previous experimental^{1,3,7–11} and theoretical^{1,12–18} reports on the additional SERS enhancement resulting from electromagnetic field localization in regions between nanoparticles or in surface cavities/pores (with negative curvature). However, the specific optimal pore size of ~ 250 nm, revealed in the present study, is unexpected. For example, several previous experimental observations^{8,10} and theoretical calculations^{8,14} for isolated (but electromagnetically coupled) nanoparticles have suggested that SERS enhancement generally increases with decreasing average interparticle distance. Such results for nanoparticles, however, cannot be directly applied for a complex coupled system such as *np*-Au. Somewhat more relevant calculations for a 2D lattice of buried spherical voids recently reported by Teperik et al.¹⁷ have shown that there are optimal conditions for the most favorable light–plasmon coupling which depend on the properties of the metal, the dielectric filling the pores as well as the size, shape, and geometrical arrangement of nanovoids. Hence, theoretical studies taking into account the specific morphology of *np*-Au (illustrated in Fig. 1) are currently needed in order to explain the pore size dependence reported here.

It should be noted that the scatter in effective SERS enhancement factors for different areas of the same sample, as clearly illustrated in Fig. 4, is not unexpected. Indeed, most of the signal from *np*-Au appears to orig-

inate from so called “hot spots” whose size, according to a very recent report by Dixon,¹⁹ is comparable with the laser beam spot size used in our experiments (ideally, ~ 2 μ m, estimated based on the parameters of the microscope objective used). The appearance of such hot spots is also consistent with a relatively wide pore size distribution in *np*-Au (see the inset in Fig. 2) and the fact that the irregular, nanoscale morphology of the *np*-Au surface could result in complex patterns of electromagnetic field enhancement.¹

Finally, SERS cross sections and, hence, SERS enhancement factors can be estimated by comparing the intensities of the methanol Raman peak at ~ 1035 cm^{-1} and a CV SERS band at ~ 1175 cm^{-1} . In such estimations, we take into account that all methanol molecules from the probed volume (whose minimum bound of ~ 60 femtoliters is estimated as the volume of a cylinder with the length equal to the depth of field and the diameter equal to the ideal beam spot size) contribute to the methanol Raman peak, while CV molecules from only a thin layer of thickness h of the solution on the *np*-Au surface contribute to the SERS signal.²⁰ Assuming that h is ~ 300 nm (which is a very conservative assumption based on experiments of Murray et al.,²¹ suggesting that h could be ~ 10 nm), one obtains enhancement factors of $\sim 10^9 - 10^{11}$ for data from Fig. 4. These numbers, however, should be viewed as a lower bound for the enhancement factors given our conservative assumptions and the existence of hot-spot effects in the SERS response of *np*-Au.¹⁹

In conclusion, we have demonstrated nanoporous Au as a highly active SERS substrate. Although as-dealloyed *np*-Au shows a weak SERS signal, subsequent thermal processing, increasing the average pore size to ~ 250 nm, dramatically improves the SERS response. This has been attributed to effects of plasmon trapping and electromagnetic field localization within pores.

We thank R. J. Anderson, C. A. Cox, J. L. Ferreira, R. T. Graff, A. M. Hodge, and E. M. Sedillo for useful discussions and/or technical assistance. This work was performed under the auspices of the U.S. DOE by the University of California, LLNL under Contract No. W-7405-Eng-48.

¹ See, for example, reviews by M. Moskovits, *Rev. Mod. Phys.* **57**, 783 (1985); A. Campion and P. Kambhampati, *Chem. Soc. Rev.* **27**, 241 (1998); *Synthesis and Plasmonic Properties of Nanostructures*, MRS Bulletin **30**, issue 5 (2005).

² K. Kneipp, Y. Wang, H. Kneipp, L. T. Perelman, I. Itzkan, R. Dasari, and M. S. Feld, *Phys. Rev. Lett.* **78**, 1667 (1997).

³ S. Nie and S. R. Emory, *Science* **275**, 1102 (1997).

⁴ R. Li and K. Sieradzki, *Phys. Rev. Lett.* **68**, 1168 (1992).

⁵ Note that the large difference between average ligament

sizes for *np*-Au samples with similar average pore sizes, illustrated in Fig. 4, is related to the fact that the surfaces of samples annealed at $400 - 600$ °C were “contaminated” with silica-containing nanoparticles, which are clearly visible as small bright spots in SEM images in Figs. 1(c) and 1(d). This effect has been observed consistently for all the foams annealed in two different tube furnaces and seems to be more pronounced when annealing is done in an O₂-containing atmosphere. Noting that the temperature required for the “development” of such nanoparticles on the *np*-Au surface coincides with the onset of a very rapid dif-

fusion of Si in Au,⁶ we attribute this effect to the outdiffusion, precipitation, and oxidation of Si impurities (in the starting alloy) during the surface-diffusion-limited evolution of Au nanofoams upon annealing. Interestingly, this initially undesirable formation of silica nanoparticles, affecting the evolution of surface morphology of nanofoams, turned out to be very useful for independently controlling the average pore and ligament sizes and helped us unravel the critical role of nanopores in the SERS response from *np*-Au. It should also be noted that the overall conclusions of this work are not affected by the presence of such silica nanoparticles since similar SERS response has been observed for both surfaces and cross sections (where no silica particles were observed) of *np*-Au with the same average pore sizes.

- ⁶ See, for example, A. K. Green and E. Bauer, *J. Appl. Phys.* **47**, 1284 (1976).
- ⁷ A. M. Michaels, J. Jiang, and L. Brus, *J. Phys. Chem. B* **104**, 11965 (2000).
- ⁸ L. Gunnarsson, E. J. Bjerneld, H. Xu, S. Petronis, B. Kasemo, and M. Kall, *Appl. Phys. Lett.* **78**, 802 (2001).
- ⁹ B. Nikoobakht and M. A. El-Sayed, *J. Phys. Chem. A* **107**, 3372 (2003).
- ¹⁰ Z. Zhu, T. Zhu, and Z. Liu, *Nanotechnology* **15**, 357 (2004).
- ¹¹ S. Coyle, M. C. Netti, J. J. Baumberg, M. A. Ghanem, P. R. Birkin, P. N. Bartlett, and D. M. Whittaker, *Phys. Rev. Lett.* **87**, 176801 (2001); J. J. Baumberg, T. A. Kelf, Y. Sugawara, S. Cintra, M. E. Abdelsalam, P. N. Bartlett, and A. R. Russell, *Nano Lett.* **5**, 2262 (2005).
- ¹² E. V. Albano, S. Daiser, G. Ertl, R. Miranda, K. Wandelt, and N. Garcia, *Phys. Rev. Lett.* **51**, 2314 (1983).
- ¹³ H. Seki, T. J. Chuang, J. F. Escobar, H. Morawitz, and E. V. Albano, *Surface Sci.* **158**, 254 (1985).
- ¹⁴ F. J. Garcia-Vidal and J. B. Pendry, *Phys. Rev. Lett.* **77**, 1163 (1996).
- ¹⁵ E. Y. Poliakov, V. A. Markel, V. M. Shalaev, and R. Botet, *Phys. Rev. B* **57**, 14901 (1998).
- ¹⁶ J. Jiang, K. Bosnick, M. Maillard, and L. Brus, *J. Phys. Chem. B* **107**, 9964 (2003).
- ¹⁷ T. V. Teperik, V. V. Popov, and F. J. Garcia de Abajo, *Phys. Rev. B* **71**, 085408 (2005).
- ¹⁸ K. J. Webb and J. Li, *Phys. Rev. B* **73**, 073404 (2006).
- ¹⁹ M. C. Dixon, Ph.D. Thesis, Pennsylvania State University, 2005.
- ²⁰ An assumption that SERS is caused by a monolayer of CV molecules chemi- and/or physisorbed on the Au surface in the solution is not supported by our results showing that SERS intensity increases with increasing CV concentration in methanolic solutions.
- ²¹ C. A. Murray, D. L. Allara, and M. Rhinewine, *Phys. Rev. Lett.* **46**, 57 (1981).